

Chicken Bone Wastes as Precursor for C-dots in Olive Oil

Wipzar Sunu Brams Dwandaru* and Emi Kurnia Sari

Physics Education Department, Mathematics and Natural Sciences Faculty,
Universitas Negeri Yogyakarta, Jl Colombo No. 1, Karangmalang,
Depok, Sleman, Yogyakarta 55281, Indonesia

*Corresponding authors: wipsarian@uny.ac.id

Published online: 25 August 2020

To cite this article: Dwandaru, W. S. B. & Sari, E. K. (2020). Chicken bone wastes as precursor for C-dots in olive oil. *J. Phys. Sci.*, 31(2), 113–131. <https://doi.org/10.21315/jps2020.31.2.8>

To link to this article: <https://doi.org/10.21315/jps2020.31.2.8>

ABSTRACT: *The objectives of this study were to synthesise and characterise carbon nanodots (C-dots) from chicken bone wastes in olive oil. The chicken bones were collected from the wastes of local chicken meat filleting shops, which were then cleaned, dried under the sun, heated in an oven at 250°C for 2 h, and ground into powder. One gram of the powder was dispersed into 10 ml of olive oil, which was then heated in a microwave for 5 min and filtered. For characterisation purposes, five drops of the solution were mixed with 8 ml of n-hexane. The carbonisation was indicated by the colour change of the solution after the microwave heating, i.e., from yellow (pure olive oil) to concentrated dark-brownish colour (C-dots solution). The characterisations were conducted using UV-Vis, photoluminescence (PL), Fourier-transform infrared (FTIR) and scanning electron microscope (SEM) to determine the optical properties of the C-dots, whereas the viscosity and the surface tension of pure olive oil and C-dots solution were also measured. The UV-Vis result showed two absorbance peaks of C-dots solution at 234 nm and 267 nm. The PL result showed green and red emissions at 499.57 nm and 673.52 nm, respectively. The FTIR result showed functional groups of C=C and C=O, which indicate the core and surface state of C-dots, respectively. The SEM result showed a surface morphology of C-dots aggregates in the structural form of homogeneous bulks. Finally, the C-dots solution had viscosity and surface tension, which were lower than those of pure olive oil so that the C-dots solution may be better absorbed by the body tissue for biomedical applications.*

Keywords: C-dots, chicken bone wastes, olive oil, surface morphology, biomedical applications

1. INTRODUCTION

The Statistic Bureau of Indonesia reported that the average weekly consumption of broiler chicken meat per capita increases every year.¹ The increase of chicken meat consumption causes the increase of chicken bone wastes.² Chicken bone wastes are commonly thrown away because they do not have any commercial value. However, as efforts for recycling, reusing and reducing (3R) wastes are being recommended globally, chicken bone wastes have been used for various applications. One of these applications is on the renewable energy sector based on environmentally friendly methods, e.g., producing biodiesel via transesterification reaction using heterogeneous catalysts.³ Chicken (and also lamb) bone wastes have also been studied to remove fluoride wastes (defluoridation) from water with very good efficiencies of up to 99.8% (and 99.4%), respectively.⁴ Naturally, chicken bone wastes may also be applied as a precursor for producing phosphate fertilisers as bio-fertilisers.⁵

Chicken bones consist of inorganic and organic materials, as well as water. The main inorganic material is calcium phosphate or known as hydroxyapatite. Chicken bones are a source of protein as the organic materials.⁶ The dominant type of protein found in chicken bones is collagen.⁷⁻¹⁰ Collagen consists of three polypeptide chains (tropocollagen) in the form of helix with repeating pattern of Gly-X-Y where X and Y are usually filled by amino acids, such as proline and hydroxyproline.^{9,10} Amino acids contain C, N, O and H elements, where carbon nanodots (C-dots) material is successfully synthesised.¹¹ Hence, chicken bone wastes are potential as precursor for C-dots material.

C-dots are carbon nanomaterials of zero-dimension with sizes of 1 nm to 10 nm that are highly fluorescent, non-toxic and biocompatible so that they can be used in various fields such as bio-imaging, bio-sensing, drug delivery, opto-electronic and catalyst.¹¹⁻¹⁹ Research on C-dots continues to grow to date.¹⁹ Besides the many applications that have been attributed to C-dots as mentioned above, another potential attention to be studied on C-dots is their intrinsic bioactivities. This is because C-dots do not contain heavy metals; hence C-dots are environmentally friendly, which should be safe to be used for biological applications.²⁰ An attempt in this line of research is synthesising nanocomposites comprising of C-dots and hydroxyapatite (C-dots/hydroxyapatite) for various applications, such as metal ion sensing, osteogenic activities and drug carrier.²¹ The C-dots/hydroxyapatite nanocomposite also improves its fluorescence property and surface area from 42 to 79 m² g⁻¹ compared to that of blank hydroxyapatite.²² Furthermore, the C-dots/hydroxyapatite nanocomposite has also been studied for its excellent loading capacity of acetaminophen and doxorubicin, as well as bone tissue engineering.²¹⁻²³

There are various methods in synthesising C-dots including arc discharge, laser ablation and electrochemical oxidation.^{24–26} The commonly used method in producing C-dots is via hydrothermal.²⁷ However, the simplest method of C-dots synthesis is using what is known by one-pot step of heating or carbonising using, for example, a microwave.^{11,28} Moreover, the precursor materials for producing C-dots also become an active area of research. Many organic materials have been used as precursor for synthesising C-dots, e.g., orange juice, bitter apple peel, banana peel and green tea leaf residue.^{29–32} These precursor materials contain carbon atoms, which constitute the basic building blocks of C-dots. Furthermore, organic materials may also be organic wastes, e.g., chicken bones. The reuse of these materials is in accordance with the concept of green synthesis of nanomaterials. Organic wastes are abundant in nature, expensive to obtain, and an effective way in implementing the 3R principle of waste management.

Olive oil is a natural liquefied fat, which is extracted from the fruits of olive (*Olea europaeae*) tree. The tree itself has a long history of cultivation in the Mediterranean Basin, which impacted a great portion of ecology, economy and culture of the region.³³ Olive oil has two useful compounds to human life, which are oleic acid and phenols.³⁴ Oleic acid is unsaturated fat, whereas phenols are antioxidant.³⁵ Olive oil has been used to reduce the risk of osteoporotic fractures in the PREDIMED trial.³⁶ Hohmann et al. state that high phenols olive oil (HPOO) can be considered as nutraceutical in cardiovascular prevention.³⁷ Dissolving nanomaterials into olive oil has been conducted for various applications, e.g., as nanoemulsions.³⁸ Moreover, Sapra et al. has successfully synthesised monodispersed CdSe nanocrystals with olive oil (oleic acid) as a stabilising agent.³⁹ Fullerene (C₆₀) has been dissolved into olive oil and administered repeatedly with a certain dose into rats and shown that there are no toxicity dangers and, in fact, it doubled the lifespan of the rats.⁴⁰ Furthermore, olive oil has a protective role as a solvent for iron oxide nanoparticles when administered into male albino rats.⁴¹ Hence, it is clear that the use of nanomaterials in olive oil may provide significant future biomedical applications. Based on the aforementioned prospect, however, investigations concerning C-dots in olive oil are still lacking. That is why this present study is conducted, which is in accordance to the enrichment of various C-dots based materials for biomedical applications.

Here, we used chicken bone wastes to synthesise C-dots, which were then dispersed into olive oil. This study provides information concerning the preparation, synthesis and characterisation of C-dots from chicken bone wastes in olive oil via the microwave method. Hence, the objectives of this study were to synthesise and characterise the C-dots from chicken bone wastes in olive oil.

The C-dots/hydroxyapatite nanocomposite described above is obtained by combining different initial or raw materials. However, in this study, all of the raw materials, i.e., collagen and hydroxyapatite are already contained in the chicken bone wastes, which shows a unique feature of a potential precursor material for producing C-dots with interesting bioactivity properties.

2. EXPERIMENTAL

The experimental method in this study can be explained in the subsequent discussion.

2.1 Preparation of Chicken bone Wastes Powder

Chicken bone powder is prepared by mechanical method using a meat grinder. First, chicken bone wastes are collected from Indonesian local chicken meat-filleting shops. Then, the chicken bones are cleaned from the remaining meat and then dried under the sun for 2 h to decrease their water content. After that, the chicken bones are heated in an electric oven (Mitseda) at 250°C for 2 h and grinded to become powder. Then, the powder is filtered through a sieve to make sure that the powder size is homogenous. All of the equipment is provided by the Physics Laboratory, Universitas Negeri Yogyakarta, Indonesia. The preparation of the chicken bone wastes powder may be observed in Figure 1.

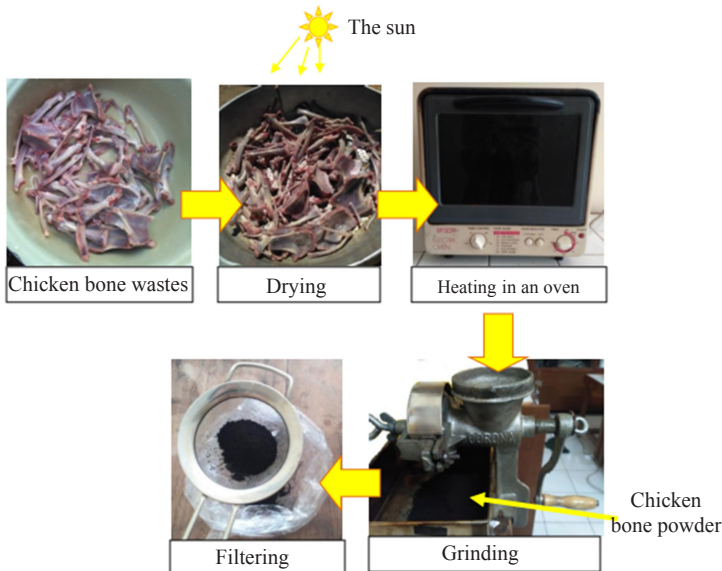


Figure 1: The preparation of chicken bone wastes powder.

2.2 Synthesis of C-dots Solution

The synthesis of the C-dots solution is straightforward and conducted by the microwave heating method. The C-dots synthesis procedure may be observed in Figure 2. An amount of 6.0 gram of chicken bone powder is dispersed in 60 ml extra virgin olive oil (Filippo Berio), purchased from an Indonesian local market, and gradually stirred. Then, the mixture is heated in a microwave oven (Sanyo EM-603MW, 1100 watts) that is provided by the Physics Laboratory, Universitas Negeri Yogyakarta for 5 min. The solution is then filtered again using a filter paper which is purchased from the Alfa Kimia (Indonesia) to separate the remaining sediment and C-dots solution. Finally, the C-dots solution is ready to be characterised.

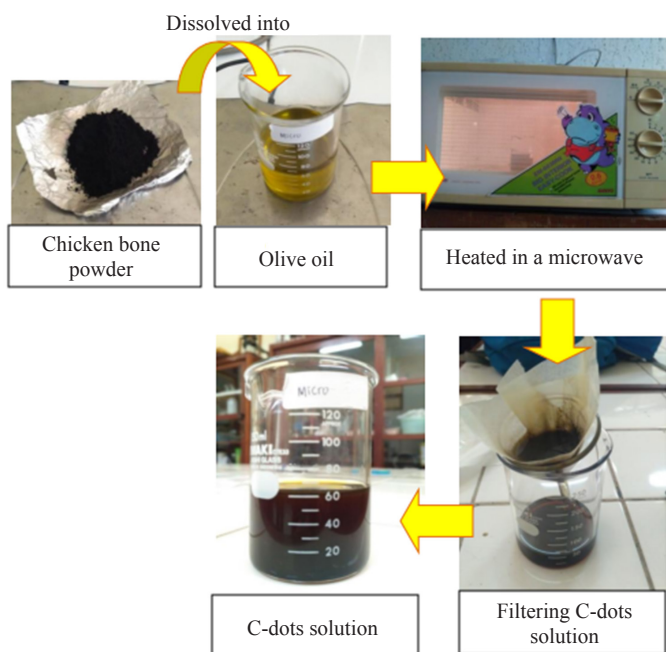


Figure 2: The C-dots synthesis procedure.

2.3 Characterisations

2.3.1 UV-Vis spectrophotometer

A UV-Vis spectrophotometer is used to determine the absorbance peaks at certain wavelengths. The wavelength ranges from 200 nm to 800 nm. This range is selected because the sample needs to be tested using UV light (200 nm to

400 nm) and visible light (400 nm to 800 nm). This characterisation is done by preparing a sample solution of 5 drops of C-dots solution mixed with 8 ml of n-hexane. The pure n-hexane solution is used for the blank solution. The UV-Vis spectrophotometer used in this study is Shimadzu UV-Vis 2450 in the Chemistry Laboratory, Universitas Negeri Yogyakarta.

2.3.2 Photoluminescence (PL) spectrophotometer

The PL is used to determine the emission of C-dots solution. The result of the PL characterisation is a graph of intensity vs. emission wavelength. This characterisation is done by preparing the sample as in the UV-Vis test, but without a blank solution. The PL device used in this study is custom-made using Ocean Optics USB 4000 Fiber Optic Spectrometer and a laser with a 405 nm excitation wavelength. Furthermore, the laser is connected to a 5 V input voltage. The spectrometer is connected to a computer, which shows the graph of intensity vs. emission wavelength. All of the equipment above is provided by Physics Laboratory, Universitas Gadjah Mada, Indonesia. The PL device may be observed in Figure 3.

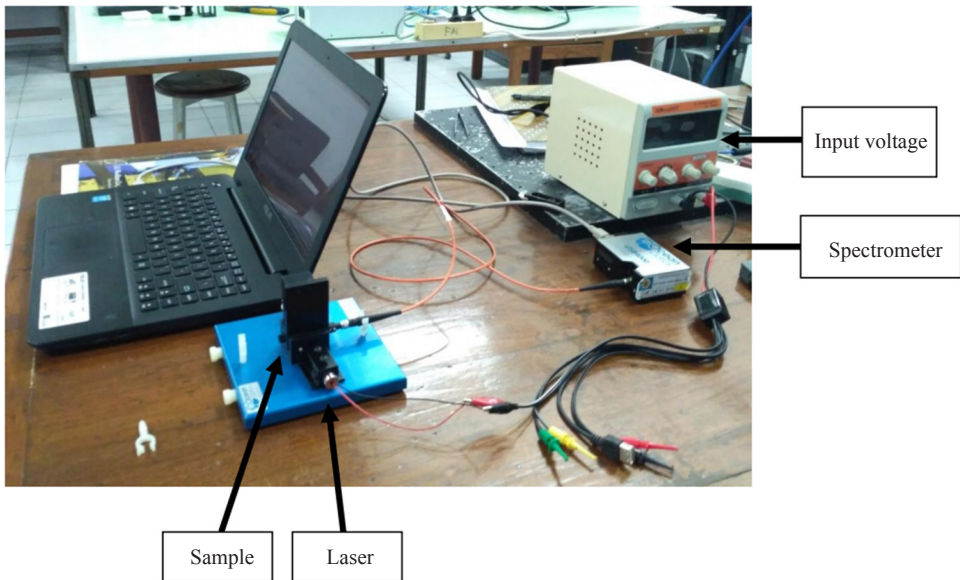


Figure 3: The PL device.

2.3.3 FTIR spectrometer

An FTIR is used to determine functional groups contained in the samples by showing the graph of transmittance vs. the wavenumber. The FTIR that is used in this research is FTIR Thermo Nicolet Avatar 360 IR provided by the Integrated Laboratory, Faculty of Mathematics and Natural Science, Indonesia Islamic University, Indonesia. This characterisation is done by directly testing the C-dots solution as the samples.

2.3.4 Scanning electron microscope (SEM)

SEM is used to determine the surface morphology of the powder. In this case, the sample for the SEM is prepared by mixing 1.0 g of chicken bone powder and 10 ml distilled water. After that, the sample is stirred gradually and filtered. The sample solution is dripped on a $1 \times 1 \text{ cm}^2$ glass slides and heated in an oven at 150°C for 10 min to become a solid sample. The SEM that is used in this study is Hitachi SU 3500 in the Indonesian Institute of Science, Indonesia.

2.3.5 Viscosity

The viscosity of the C-dots solution and pure olive oil is measured using a set of Redwood's viscometer apparatus, which can be observed in Figure 4. The Physics Laboratory, Universitas Negeri Yogyakarta, provided this equipment. The procedure in measuring the viscosity can be explained as follows: (1) weighing 50 ml C-dots solution to determine the density of the solution; (2) setting the ball valve on the orifice; (3) pouring the 50 ml C-dots solution into the oil tube; (4) pouring water into the water bath; (5) setting the thermometers on the water bath and oil tube; (6) heating the water bath; (7) after a certain temperature, starting the stopwatch and at the same time opening the ball valve so that the solution drips and goes into the beaker glass; and (8) stopping the stopwatch after the dripping ends. The data obtained from this experiment is time (second), known as the Redwood second. Hence, the kinetic viscosity may be measured via the equation:

$$v = At - \frac{B}{t} \quad (1)$$

where:

v = kinetic viscosity ($\text{m}^2 \text{s}^{-1}$),

A = viscometer constant which can be determined by equipment ($\text{m}^2 \text{s}^{-2}$),

t = Redwood second or time of flow (s), and

B = coefficient of kinetic energy (m^2).⁴²

Moreover, the dynamic viscosity can be determined using the following equation:

$$\mu = v\rho \quad (2)$$

where:

μ = dynamic viscosity (Ns m^{-2}), and
 ρ = density of the solution (kg m^{-3}).⁴³

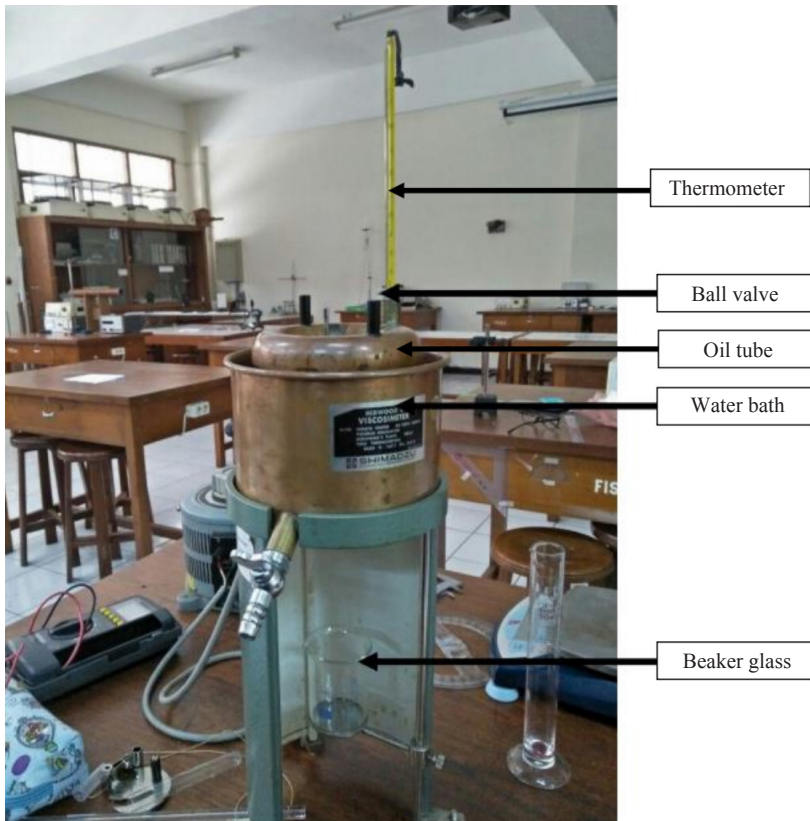


Figure 4: Redwood's viscometer.

2.3.6 Surface tension

The surface tension measurement is conducted based on the wetting of the C-dots solution upon the container's surface, which can be observed in Figure 5. The Physics Laboratory, Universitas Negeri Yogyakarta, provided the equipment in this measurement. The procedure in measuring the surface tension may be given as follows: (1) putting a ruler vertically on a measuring cup; (2) weighing 20 ml

of C-dots solution and pouring it into the measuring cup; (3) taking photographs of the C-dots solution so the concave meniscus is clearly observed, shown in Figure 5(a); and (4) determining the height of the C-dots solution at the interface with the measuring cup, shown in Figure 5(c), using the CorelDraw software. Finally, the surface tension of the C-dots solution can be determined using:

$$\gamma = \frac{\rho r y g}{2 \cos \theta} \quad (3)$$

where:

γ = surface tension (N m^{-1}),

ρ = density of the solution (kg m^{-3}),

r = radius of the measuring cup (m),

y = adhesion height (m),

g = gravity acceleration (m s^{-2}), and

θ = surface tension angle ($^{\circ}$).

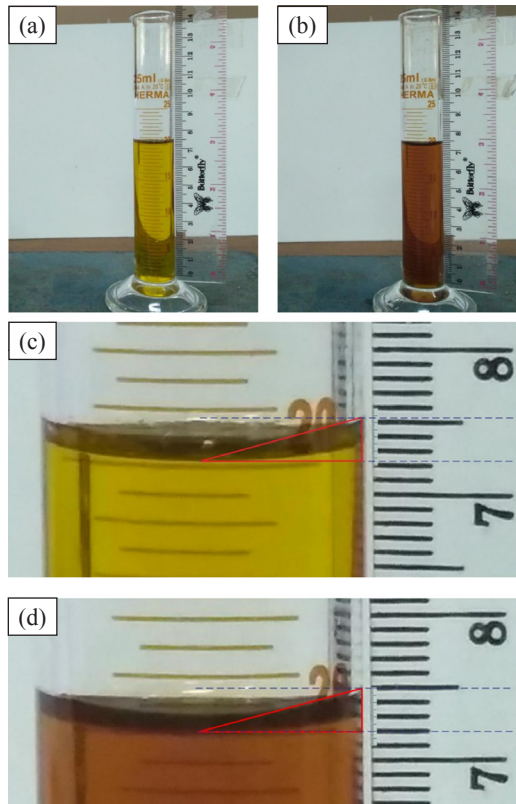


Figure 5: Surface tension measurement of olive oil (a,c) and C-dots (b,d).

3. RESULTS AND DISCUSSION

C-dots solution has been synthesised from chicken bone wastes in olive oil. The synthesis of the C-dots solution uses an oven producing a sample in the form of a solution because evaporation of the solvent (olive oil) does not occur. The C-dots (in olive oil) solutions produced in this study are given in Figure 6(b). Based on Figure 6(a), pure olive oil solution has yellow colour while C-dots solution as shown in Figure 6(b) has dark-brownish colour. The colour change of the C-dots solution after the (microwave) heating is an indication of a carbonisation process.⁴⁴ The carbonisation process also indicates that C-dots are formed. The first simple test to determine the occurrence of C-dots in the sample is by subjecting a UV laser ($\lambda_{exc} = 405 \text{ nm}$) through the sample, which is shown in Figure 6(c). Figure 6(c) shows the luminescence of the C-dots solution when it is given a UV laser.

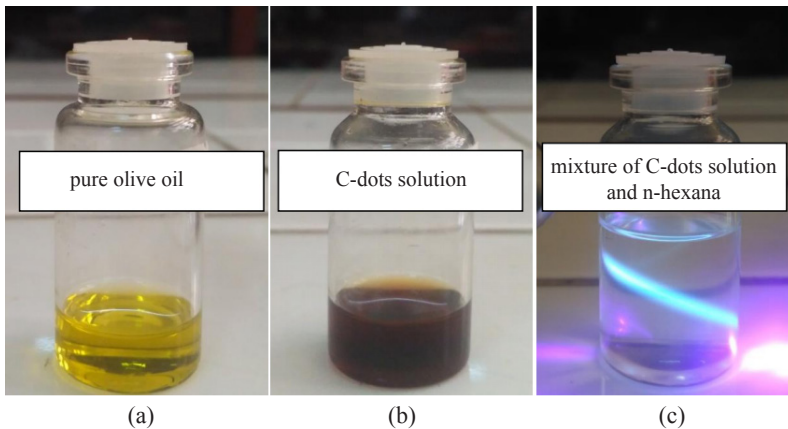


Figure 6: Various solutions in this study, i.e., (a) pure olive oil, (b) C-dots solution, and (c) mixture of C-dots solution and n-hexane being subjected to a UV laser.

Figure 7(a) shows the UV-Vis results of C-dots and olive oil. The C-dots and olive oil samples have two absorbance peaks, respectively. The sample of olive oil has absorbance peaks at wavelengths of 231 nm and 267 nm, and a sharp decrease of the absorbance after the shouldering peak. Moreover, the C-dots sample has two absorbance peaks as well at wavelengths of 234 nm and 267 nm with a tail that is extended to higher visible wavelengths. These absorbance peaks indicate the existence of two electronic transitions or excitations.⁴⁵ The transition of the first and second peaks are $\pi \rightarrow \pi^*$ and $n \rightarrow \pi^*$, respectively.⁴⁶ One or two absorbance peaks with absorbance profile extending to higher visible wavelengths indicates the formation of C-dots.^{15,47} Hence, the above UV-Vis results show differences between the C-dots solution and olive oil in their absorbance properties. There is a redshift on the first absorbance peak of the olive oil and C-dots, i.e., from

231 nm to 234 nm. Besides, the C-dots have a long tail extending to higher visible wavelengths, whereas the olive oil undergoes a sharp drop after the shouldering peak. Finally, the absorbance value of the C-dots is higher compared to that of the olive oil, especially at the shouldering peak.

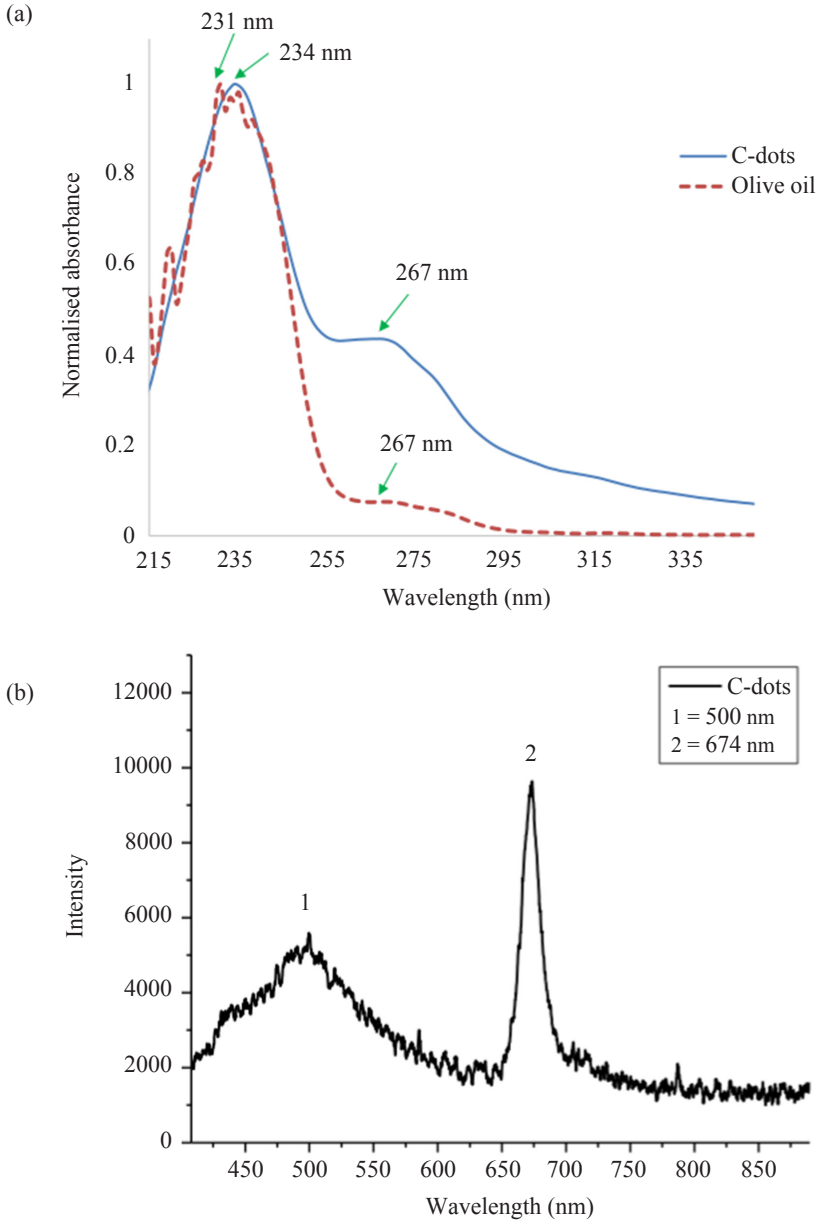


Figure 7: The characterisation results of the C-dots solution using (a) UV-Vis, and (b) PL.

Further characterisation is provided by PL, which is related to the electronic transitions from excited to ground states using a UV laser of 405 nm as the excitation wavelength. The PL spectrum shows a relation between the intensity and emission wavelength given in Figure 7(b). The PL spectrum of Figure 7(b) has two intensity peaks with different emission wavelengths, i.e., 499.57 nm and 673.52 nm. The emission at 499.57 nm indicates a green wavelength (495–770 nm) so that the C-dots solution produced emits green light.^{45,46} According to literature, the second peak at 673.52 nm shows a structure of porphyrin, which is a part of many structures of chlorophyll.^{45,48} In this case, the porphyrin comes from the olive oil because olive oil contains chlorophyll compounds. According to a study, extra virgin olive oil has a high intensity peak at wavelengths in the range of 650 nm to 730 nm and is relatively flat at other wavelengths.⁴⁹ The aforementioned peak is of course in accordance with the second peak of the PL spectrum in Figure 7(b), which shows the porphyrin structure in the olive oil as the dominant compound.

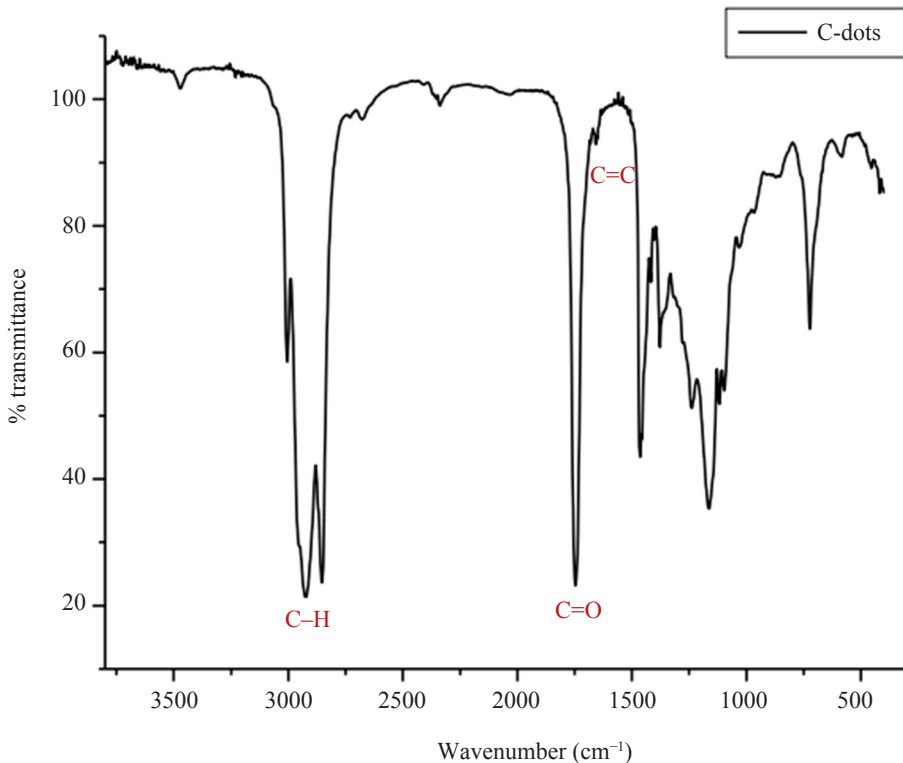


Figure 8: FTIR result of the C-dots solution sample.

The next characterisation is the FTIR to determine the functional groups in the C-dots solution, which is depicted in Figure 8. The result of the FTIR is the transmittance vs. wavenumber. Each functional group corresponds to a certain wavenumber that depends on its ability to vibrate and absorb energy from the IR spectrum. Based on Figure 8, the functional groups that can be identified in the sample are C-H, C=O and C=C. The presence of C=C bond at 1654.71 cm^{-1} indicates the occurrence of the C-dots material. Although it is a weak transmittance peak, the C=C bond forms the core of C-dots.⁴⁴ The functional groups of C-H and C=O have sharp transmittance peaks at 2923.99 cm^{-1} and 1746.75 cm^{-1} , respectively. The oxygen functional group of C=O shows the surface state of the C-dots material. Based on the FTIR result of olive oil conducted, the functional groups found in olive oil consist of C=O, C-H and O-H.⁵⁰ The C=O and C-H functional groups are also found in the C-dots sample in Figure 8. However, there are differences between these FTIR results. Hydroxyl (O-H) functional groups are not detected in the C-dots sample in Figure 8, whereas C=C functional groups are not detected in olive oil. This shows that olive oil has a very low intensity of C=C groups detected by the FTIR. Hence, the C=C groups in Figure 8 should be the result of the existing C-dots in the sample.

We may compare the UV-Vis and FTIR results of the samples obtained in this study. Based on the UV-Vis result, the C-dots sample has two absorbance peaks that indicate the core and the surface state of C-dots, respectively. On the other hand, the FTIR test produces two functional groups, i.e., C=C and C=O. The C=C and C=O functional groups also indicate the core and the surface state of the C-dots, respectively. Hence, the result of UV-Vis test is in accordance with the FTIR test and mutually reinforces that the resulting sample obtained is C-dots.

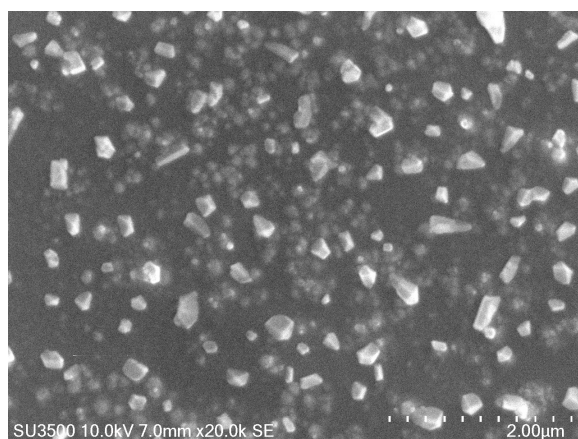


Figure 9: The SEM image of the C-dots with 20000X magnification.

The next characterisation is using the SEM to determine the surface morphology of the C-dots solution. The SEM of the C-dots solution is a result of the chicken bone powder dispersed in water not in olive oil. This can be observed in Figure 9, which shows aggregates of C-dots in the structural form of bulks. However, these bulks are not particles of C-dots, but they consist of many C-dots particles.⁵¹ These bulks spread homogenously on the SEM testing area. The result of the SEM test also shows that the position of the bulks is determined by their brightness. The bulks that are in a higher position appear brighter.

Table 1: Density, viscosity and surface tension of pure olive oil and C-dots solution.

Sample	Density (kg m ⁻³)	Viscosity (Ns m ⁻²)	Surface tension (N m ⁻¹)
C-dots solution	765	8.6×10^{-4}	5.93
Olive oil	865	9.6×10^{-4}	6.37

Furthermore, the measurement results of the viscosity and surface tension of the C-dots solution may be observed in Table 1. It may be clearly seen that the density, viscosity and surface tension of C-dots solution is lower than the pure olive oil. This indicates that the addition of C-dots into the olive oil decreases the values of the viscosity and surface tension of the olive oil. In the heating process of the solution using the microwave, the microwave makes the molecules of the solution to vibrate and interact with each other.⁵² The C-dots particles fill the spaces between the olive oil molecules, hence reducing the cohesion forces of the olive oil molecules. This causes the decrease of the viscosity and also the surface tension. The decrease in the viscosity makes the C-dots solution flow more easily, whereas the decrease of the surface tension makes the C-dots solution easier to interact with the interface material. On the other hand, the olive oil also acts as a stabiliser for the C-dots particles.³⁹ Hence, there are mutual advantages between the C-dots particles and olive oil, which make the C-dots (in olive oil) solution a prospective candidate for biomedical applications.

4. CONCLUSION

C-dots have been synthesised from chicken bone wastes in olive oil via the microwave heating method. The carbonisation is indicated by the colour change of the solution after the microwave heating, i.e., from yellow (pure olive oil) to concentrated dark-brownish (C-dots solution). The C-dots solution has two absorbance peaks at the wavelengths of 234 nm and 267 nm. The C-dots solution emits green luminescent, whereas the red luminescent comes from the chlorophyll of the olive oil. The UV-Vis results are in accordance to the FTIR results that the C-dots solution has a core and surface state which are shown by the existence of

C=C and C=O functional groups, respectively. The SEM image shows aggregates of C-dots and hydroxyapatite particles in bulks. The viscosity and surface tension of the C-dots solution are lower than those of the pure olive oil. These properties may be used to further explore the C-dots solution for various biomedical applications. The individual C-dots particle is not observed in the SEM image. Therefore, in order to obtain the size and morphology images of the C-dots particles, further characterisations, using SEM-XRF, transmission electron microscope (TEM) or high resolution TEM (HR-TEM) should be conducted. The size of the C-dots may also be analysed via the Tauc plot based on the UV-Vis data results as explained in a study.⁵³ In this study, we have not yet attempted to separate the C-dots from the olive oil, as it is not our main concern. However, this may be conducted in future studies to obtain the gain of the C-dots from the chicken bone wastes.

5. ACKNOWLEDGEMENTS

The authors would like to thank the Physics Education Department, Faculty of Mathematics and Natural Science, Universitas Negeri Yogyakarta for funding this study through the 2019 Research Group scheme with the grant No. B/144/UN34.13/PM.01.00/2019. We also would like to express our gratitude to Bambang Sugeng, PhD from the English Literature Department, Universitas Negeri Yogyakarta for proofreading this manuscript.

6. REFERENCES

1. Statistics Bureau of Indonesia. (2019). The average per capita consumption a week of several important foodstuffs. Retrieved 20 June 2019 from <https://www.bps.go.id/statictable/2014/09/08/950/rata-rata-konsumsi-per-kapita-seminggu-beberapa-macam-bahan-makanan-penting-2007-2017.html>.
2. Rugayah, N. et al. (2014). Chicken bone charcoal for defluoridation of groundwater in Indonesia. *Int. J. Poult. Sci.*, 13(10), 591–596. <https://doi.org/10.3923/ijps.2014.591.596>
3. Farooq, M., Ramli, A. & Naeem, A. (2015). Biodiesel production from low FFA waste cooking oil using heterogeneous catalyst derived from chicken bones. *Renew. Energy*, 76, 362–368. <https://doi.org/10.1016/j.renene.2014.11.042>
4. Ismail, Z. Z. & AbdelKareem, H. N. (2015). Sustainable approach for recycling waste lamb and chicken bones for fluoride removal from water followed by reusing fluoride-bearing waste in concrete. *Waste Manage.*, 45, 66–75. <https://doi.org/10.1016/j.wasman.2015.06.039>
5. Ferreira dos Santos, C. M., Narciso, C. M. & Soares, I. R. (2020). Analysis of heat treatment of chicken bones for the obtaining of phosphate biofertilizer. *Braz. J. Dev.*, 6(3), 14288–14296. <https://doi.org/10.34117/bjdv6n3-337>

6. Centenaro, G. S., Mellado, M. S. & Prentice-Hernández, C. (2011). Antioxidant activity of protein hydrolysates of fish and chicken bones. *Adv. J. Food. Sci. Technol.*, 3(4), 280–288.
7. Yuliani, D. et al. (2019). Effect of phosphoric acid pretreatment on characterization of gelatin from broiler chicken (*Gallus gallus domesticus* L.) bones. Paper presented at the IOP Conference Series: Earth and Environmental Science, Surabaya, 23–24 August. <https://doi.org/10.1088/1755-1315/293/1/012013>
8. Hashim, P. et al. (2015). Collagen in food and baverage industries. *Int. Food Res. J.*, 22(1), 1–8.
9. Liu, D. et al. (2012). Extraction and characterization of pepsin-solubilised collagen from fins, scales, skins, bones and swim bladders of bighead carp (*Hypophthalmichthys nobilis*). *Food Chem.*, 133, 1441–1448. <https://doi.org/10.1016/j.foodchem.2012.02.032>
10. Silvipriya, K. S. et al. (2015). Collagen: Animal sources and biomedical application. *J. Appl. Pharm.*, 5(3), 123–127. <https://doi.org/10.7324/JAPS.2015.50322>
11. Jiang, J. et al. (2012). Amino acids as the source for producing carbon nanodots: microwave assisted one-step synthesis, intrinsic photoluminescence property and intense chemiluminescence enhancement. *Chem. Commun.*, 48(77), 9634–9636. <https://doi.org/10.1039/c2cc34612e>
12. Baker, S. N. & Baker, G. A. (2010). Luminescent carbon nanodots: Emergent nanolights. *Angew. Chem. Int. Ed.*, 49(38), 6726–6744. <https://doi.org/10.1002/anie.200906623>
13. Wang, Y. & Hu, A. (2014). Carbon quantum dots: Synthesis, properties and applications. *J. Mater. Chem. C.*, 2(34), 6921–6939. <https://doi.org/10.1039/c4tc00988f>
14. Bao, L. et al. (2015). Photoluminescence-tunable carbon nanodots: Surface-state energy-gap. *Adv. Mater.*, 27(10), 1663–1667. <https://doi.org/10.1002/adma.201405070>
15. Soni, S. & Maria, A. L. (2016). *Luminescent carbon dots: Characteristics and applications*. Master diss., University of Groningen, the Netherlands.
16. Liu, H., Ye, T. & Mao, C. (2007). Fluorescent carbon nanoparticles derived from candle soot. *Angew. Chem. Int. Ed.*, 46(34), 6473–6475. <https://doi.org/10.1002/anie.200701271>
17. Zhang, J. et al. (2010). Controlled synthesis of green and blue luminescent carbon nanoparticles with high yields by the carbonization of sucrose. *New J. Chem.*, 34(4), 591–593. <https://doi.org/10.1039/B9NJ00662A>
18. Yang, S.-T. et al. (2009). Carbon dots for optical imaging in vivo. *J. Am. Chem. Soc.*, 131(32), 11308–11309. <https://doi.org/10.1021/ja904843x>
19. Liu, X.-J. et al. (2013). Improved fluorescence of carbon dots prepared from bagasse under alkaline hydrothermal conditions. *BioRes.*, 8(2), 2537–2546. <https://doi.org/10.15376/biores.8.2.2537-2546>
20. Zhang, M. et al. (2018). Novel carbon dots derived from Schizonepetae Herba Carbonisata and investigation of their haemostatic efficacy. *Artif. Cells Nanomed. Biotechnol.*, 46(8), 1562–1571. <https://doi.org/10.1080/21691401.2017.1379015>

21. Sarkar, C. et al. (2018). One pot synthesis of carbon dots decorated carboxymethyl cellulose-hydroxyapatite nanocomposite for drug delivery, tissue engineering and Fe³⁺ ion sensing. *Carbohydr. Polym.*, 181, 710–718. <https://doi.org/10.1016/j.carbpol.2017.11.091>
22. Chung, H. K. et al. (2019). Biowaste-derived carbon dots/hydroxyapatite nanocomposite as drug delivery vehicle for acetaminophen. *J. Sol-Gel Sci. Techn.*, 93, 214–223. <https://doi.org/10.1007/s10971-019-05141-w>
23. Gogoi, S. et al. (2016). A renewable resource-based carbon dot decorated hydroxyapatite nanohybrid and its fabrication with waterborne hyperbranched polyurethane for bone tissue engineering. *RSC Adv.*, 6(31), 26066–26076. <https://doi.org/10.1039/C6RA02341J>
24. Dey, S. et al. (2014). Luminescence properties of boron and nitrogen doped graphene quantum dots prepared from arc-discharge-generated doped grapheme samples. *Chem. Phys. Lett.*, 595–596, 203–208. <https://doi.org/10.1016/j.cplett.2014.02.012>
25. Russo, P. et al. (2014). Femtosecond laser ablation of highly oriented pyrolytic graphite: A green route for large-scale production of porous graphene and graphene quantum dots. *Nanosci.*, 6(4), 2381–2389. <https://doi.org/10.1039/C3NR05572H>
26. Ming, H. et al. (2012). Large scale electrochemical synthesis of high quality carbon nanodots and their photocatalytic property. *Dalton Trans.*, 41(31), 9526–9531. <https://doi.org/10.1039/C2DT30985H>
27. Lu, Y. et al. (2018). Facile hydrothermal synthesis of carbon dots (CDs) doped ZnFe₂O₄/TiO hybrid materials with high photocatalytic activity. *J. Photochem. Photobio. A.*, 353, 10–18. <https://doi.org/10.1016/j.jphotochem.2017.10.049>
28. Zhai, X. et al. (2012). Highly luminescent carbon nanodots by microwave-assisted pyrolysis. *Chem. Commun.*, 48(64), 7955–7957. <https://doi.org/10.1039/C2CC33869F>
29. Sahu, S. et al. (2012). Simple one-step synthesis of highly luminescent carbon dots from orange juice: Application as excellent bio-imaging agents. *Chem. Commun.*, 48(70), 8835–8837. <https://doi.org/10.1039/C2CC33796G>
30. Aggarwal, R. et al. (2020). Bitter apple peel derived photoactive carbon dots for the sunlight induced photocatalytic degradation of crystal violet dye. *Sol. Energy*, 197, 326–331. <https://doi.org/10.1016/j.solener.2020.01.010>
31. Atchudan, R. et al. (2020). Hydrophilic nitrogen-doped carbon dots from biowaste using dwarf banana peel for environmental and biological applications. *Fuel*, 275, 1–10. <https://doi.org/10.1016/j.fuel.2020.117821>
32. Hu, Z. et al. (2020). The N, S co-doped carbon dots with excellent luminescent properties from green tea leaf residue and its sensing of gefitinib. *Microchem. J.*, 154(104588), 1–8. <https://doi.org/10.1016/j.microc.2019.104588>
33. Arenas-Castro, S. et al. (2020). Projected climate changes are expected to decrease the suitability and production of olive varieties in southern Spain. *Sci. Total Environ.*, 709(136161), 2–47. <https://doi.org/10.1016/j.scitotenv.2019.136161>
34. Martinez, S. B. & Valcarcel, M. (2014). Graphene quantum dots as sensor for phenols in olive oil. *Sens. Act. B Chem.*, 197, 350–357. <https://doi.org/10.1016/j.snb.2014.03.008>

35. Carrasco-Pancorbo, A. et al. (2005). Analytical determination of polyphenols in olive oils. *J. Sep. Sci.*, 28(9–10), 837–858. <https://doi.org/10.1002/jssc.200500032>
36. Gracia-Gavilan, J. F. et al. (2016). Extra virgin olive oil consumption reduces the risk of osteoporotic fractures in PREDIMED trial. *Clin. Nutr.*, 37(1), 329–335. <https://doi.org/10.1016/j.clnu.2016.12.030>
37. Hohmann, C. D. et al. (2015). Effects of high phenolic olive oil on cardiovascular risk factor: A systemic review and meta-analysis. *Phytomed.*, 22(6), 631–640. <https://doi.org/10.1016/j.phymed.2015.03.019>
38. Wang, X. et al. (2016). Carbon-based nanomaterials for nanozymes. In Wang, X. (Eds.). *Nanozymes: Next wave of artificial enzymes*. Berlin: Springer, 7–29.
39. Sapra, S., Rogach, A. L. & Feldmann, J. (2006). Prosphine-free synthesis of monodisperse CdSe nanocrystals in olive oil. *J. Mater. Chem.*, 16(33), 391–395. <https://doi.org/10.1039/B607022A>
40. Baati, T. et al. (2012). The prolongation of the lifespan of rats by repeated oral administration of [60] fullerene. *Biomater.*, 33(19), 4936–4946. <https://doi.org/10.1016/j.biomaterials.2012.03.036>
41. Shakra, M. E. et al. (2019). Hepatotoxicity of bare and polyethylene glycol coated iron oxide nanoparticles and the protective role of virgin olive oil in male albino rats. *Egypt. J. Hosp. Med.*, 76(2), 3607–3617. <https://doi.org/10.12816/EJHM.2019.39169>
42. Boda, M. A. et al. (2015). Analysis of kinematic viscosity for liquids by varying temperature. *Int. J. Innov. Res. Sci. Eng. Technol.*, 4(4), 1951–1954. <https://doi.org/10.15680/IJIRSET.2015.0404020>
43. Simpson, D. A. (2017). Surface engineering concepts. In Simpson, D. A. (Ed.). *Practical onshore gas field engineering*. New York: Gulf Professional Publishing, 222–223.
44. Dwandaru, W. S. B. et al. (2019). Optical properties comparison of carbon nanodots synthesized from commercial granulated sugar using hydrothermal method and microwave. *Mater. Res. Express.*, 6(10), 1–8. <https://doi.org/10.1088/2053-1591/ab3952>
45. Dwandaru, W. S. B. et al. (2020). Cdots and Cdots/S synthesis from nam-nam fruit (*Cynometra cauliflora* L.) via frying method using cooking oil. *Dig. J. Nanomater. Bios.*, 15(2), 555–560.
46. Mewada, A. et al. (2015). Non-blinking dendritic crystal from C-dots solution. *Carbon Lett.*, 16(3), 211–214.
47. De, B. & Karak, N. A. (2013). Green and facile approach for the synthesis of water-soluble fluorescent carbon dots from banana juice. *RSC Adv.*, 3(22), 8286–8290. <https://doi.org/10.1039/C3RA00088E>
48. Li, L. et al. (2017). In situ synthesis of NIR-light emitting carbon dots derived from spinach for bio-imaging applications. *J. Mater. Chem. B*, 5(35), 7328–7334. <https://doi.org/10.1039/C7TB00634A>
49. Sena, A. W., Isnaeni & Juliastuti, E. (2017). Optical characterization of major compounds in different types of commercial olive oil using photoluminescence method. *Proced. Eng.*, 170, 357–362. <https://doi.org/10.1016/j.proeng.2017.03.053>

50. Labidi, N. S. & Iddou, A. (2007). Adsorption of oleic acid on quartz water interface. *J. Saudi Chem. Soc.*, 11(2), 221–234.
51. Zhang, H. et al. (2012). Carbon quantum dots/Ag₃PO₄ complex photocatalytic with enhanced photocatalytic activity and stability under visible light. *J. Mater. Chem.*, 22(21), 10501–10506. <https://doi.org/10.1039/c2jm30703k>
52. Yoshikawa, N. (2020). Mechanism of microwave heating of matter. In Horikoshi, S. & Serpone, N. (Eds.). *RF power semiconductor generator application in heating and energy utilization*. Singapore: Springer, 71–89.
53. Nuryantini, A. Y. et al. (2017). Do it yourself: Optical spectrometer for physics undergraduate instruction in nanomaterial characterization. *Eur. J. Phys.*, 38(5), 1–9. <https://doi.org/10.1088/1361-6404/aa7dbb>